Influence of laser pulse characteristics on the hot electron contribution to the third-order nonlinear optical response of gold nanoparticles

Yannick Guillet,[1] Majid Rashidi-Huyeh,[1,2] and Bruno Palpant[1,*]
[1]*INSP, CNRS UMR 7588, Université Pierre et Marie Curie–Paris 6, Campus Boucicaut, 140 rue de Lourmel, Paris F-75015, France*
[2]*Department of Physics, University of Sistan and Baluchestan, 98135-674 Zahedan, Iran*
(Received 6 June 2008; revised manuscript received 11 December 2008; published 13 January 2009)

The third-order nonlinear optical response of noble-metal nanoparticles embedded in a dielectric matrix depends on the particle intrinsic third-order susceptibility $\chi_m^{(3)}$. We propose a model which allows one to calculate the hot electron contribution $\chi_{\mathrm{he}}^{(3)}$ to $\chi_m^{(3)}$ in the case of gold. This phenomenon stems from the modification of the conduction-electron distribution induced by an optical excitation, and is significant when picosecond or subpicosecond laser pulses are considered. We show, in the case of a weak perturbation, the importance of the athermal regime for pulse widths lower than about 1 ps. Applying this model to two different samples, we then highlight the strong influence of the linear optical properties of the material on the spectral dispersion of $\chi_{\mathrm{he}}^{(3)}$. Finally, the variation in $\chi_{\mathrm{he}}^{(3)}$ with intensity in the high excitation regime is discussed for picosecond pulses.

DOI: 10.1103/PhysRevB.79.045410 PACS number(s): 78.67.Bf, 42.65.Re

I. INTRODUCTION

Confinement of noble metals at the nanometric scale gives rise to materials with novel optical properties, the main origin of which being the so-called surface-plasmon resonance (SPR).[1] This phenomenon results in the amplification of the local electric field inside and around the nanoparticles. A resonance band thus appears in the absorption spectrum of the nanocomposite material. This specific linear optical response has given birth during the last decade to applications in various fields such as photocatalysis,[2] photonics,[3] optical data storage,[4] photothermal cancer therapy,[5] biological imaging,[6] or industrial painting.[7] Furthermore, the local-field enhancement leads to a stronger nonlinear optical response than the one of metal in its bulk phase, as was shown in the pioneering work of Hache *et al.*[8,9] Hence, the large optical Kerr susceptibility of materials containing noble-metal nanoparticles has aroused the interest of several groups for two decades now and seems to enable new photonic applications. However, most of the studies consist essentially of experimental investigations based on either z-scan or degenerate four-wave mixing (DFWM).[10,11] In parallel, only a few theoretical works have been realized.[12–14] Let us mention the work of Shalaev[15] in the case of semicontinuous metal films.

The optical Kerr effect results in the creation in the medium of a third-order nonlinear polarization $P^{(3)}$ at the same circular frequency ω as the one of the applied electric field E_0. $P^{(3)}$ is related to the field E through the third-order susceptibility $\chi^{(3)}$,[16]

$$P^{(3)}(\omega) = 3\epsilon_0 \chi^{(3)}(\omega)|E(\omega)|^2 E(\omega), \tag{1}$$

where ϵ_0 is the permittivity of vacuum. In this expression, if E is linearly polarized along the x axis, $\chi^{(3)}(\omega)$ is a simplified notation standing for the fourth-rank tensor $\chi_{xxxx}^{(3)}(-\omega;\omega,\omega,-\omega)$.

Equation (1) is valid as far as it is applied to a homogeneous medium. However, extending the concept of effective medium to the nonlinear optical properties, the optical Kerr effect in a nanocomposite material can be described in the quasistatic approximation by an effective nonlinear susceptibility $\chi_{\mathrm{eff}}^{(3)}$.[14] In the case of gold nanoparticles in an amorphous oxide matrix the nonlinear susceptibility of metal has a modulus much larger than the one of the dielectric medium (respectively, $\sim 10^{-8}$ and $\sim 10^{-14}$ esu).[17–19] We also assume that the particle intrinsic third-order susceptibility $\chi_m^{(3)}$ is the same for all nanoparticles. Furthermore, the electric field inside nanoparticles is supposed to be homogeneous. In the case of a dilute medium and under these assumptions, $\chi_{\mathrm{eff}}^{(3)}$ can be written as[20]

$$\chi_{\mathrm{eff}}^{(3)} = p f_l^2 |f_l|^2 \chi_m^{(3)}, \tag{2}$$

where p and f_l denote, respectively, the metal volume fraction and the local-field factor. In the high dilution limit, the latter is identified to be the local-field factor of an isolated metal sphere,

$$f_l = \frac{3\epsilon_d}{\epsilon + 2\epsilon_d}, \tag{3}$$

where ϵ_d (ϵ) is the dielectric function of the matrix (the metal). Equation (2) brings out the dependence of $\chi_{\mathrm{eff}}^{(3)}$ on the morphology of the medium, through f_l: $|\chi_{\mathrm{eff}}^{(3)}| \sim |f_l|^4$. f_l being resonant at the SPR, i.e., $|f_l| > 1$, we see from Eq. (2) that the confinement of gold at a nanometric scale results in the strong enhancement of the optical Kerr effect at resonance. But Eq. (2) reveals also the dependence of $\chi_{\mathrm{eff}}^{(3)}$ on the intrinsic nonlinear optical properties of the metal nanoparticles, $\chi_m^{(3)}$.

In this paper, we will focus on this last parameter, which has not been theoretically investigated since the pioneering works of Flytzanis and co-workers.[8,9,20] They invoked, in the case of noble metals, three different contributions to the value of $\chi_m^{(3)}$. In addition to the usual intraband ($\chi_{\mathrm{intra}}^{(3)}$) and interband ($\chi_{\mathrm{inter}}^{(3)}$) contributions (corresponding to transitions within the *sp* band and from the *d* bands to the *sp* band, respectively), they considered a third one called the *hot electron* contribution. When the energy of the laser pulse is absorbed by nanoparticles, their conduction-electron distribution f is modified in the vicinity of the Fermi level, resulting in an increase in the electron-gas temperature. For a suffi-

ciently high incident intensity and when the pulse duration is less than a few picoseconds, the optical transition spectrum can thus be strongly modified.[21] Even if the hot electron phenomenon is not a pure electronic nonlinear effect, contrary to the intraband and interband contributions, Hache *et al.*[9] showed that it can be added as a third contribution, $\chi_{\mathrm{he}}^{(3)}$, to the particle susceptibility $\chi_m^{(3)}$. Their calculation was restricted to photon energies close to the SPR, in the low perturbation regime and for 5 ps pulses. However, their results have often been taken for granted in a much larger range of experimental situations. The validity of such generalizations has up to now never been assessed.

In this paper, we theoretically investigate the hot electron contribution to the intrinsic third-order nonlinearity of a gold nanoparticle over a wide spectral range, varying both the pulse width and the excitation magnitude. In a first part, we expose the theoretical model we use to evaluate the dynamics of f following an optical excitation and the resulting modification of the optical transition spectrum. We then define $\chi_{\mathrm{he}}^{(3)}$ in the framework of the optical Kerr effect formalism. In a second part, we successively discuss the pulse width, wavelength, and intensity dependences of the nonlinear optical response. The consequences are illustrated on two samples having different linear optical properties and we compare our theoretical predictions to results found in the literature.

II. CALCULATION OF $\chi_{\mathrm{he}}^{(3)}$

A. Experimental parameters for the calculation

We will present in this section the theoretical approach used to determine the hot electron contribution to $\chi_m^{(3)}$. We consider the laser pulse excitation of gold nanoparticles embedded in a dielectric matrix. The pulse is characterized by a duration τ_p (defined as the full width at half maximum of the instantaneous power), ranging from a few hundreds of femtoseconds to a few picoseconds, by a photon energy $\hbar\omega_p$ and by a peak intensity I_0.

The instantaneous power absorbed by metal volume unit, $P_{\mathrm{abs}}(t)$, is the relevant parameter for describing the excitation magnitude. It has the temporal shape of the laser pulse, which we assume to be a Gaussian peaked at t_0,

$$P_{\mathrm{abs}}(t) = P_0 \exp\left[-\ln 16\left(\frac{t-t_0}{\tau_p}\right)^2\right]. \tag{4}$$

As the nanoparticle size is much smaller than the beam waist, no any spatial dependence of P_{abs} will be considered. In the case of a thin nanocomposite film, P_0 is linked with the experimental parameter I_0 through

$$P_0 = \frac{I_0 T_{\mathrm{af}}(1-e^{-\alpha_f L})}{pL}, \tag{5}$$

where T_{af} is the light intensity transmittance of the air-film interface, α_f is the film absorption coefficient, L is the film thickness, and p is its metal volume fraction. In the case of weak total absorption ($\alpha_f L \ll 1$), Eq. (5) simplifies as

$$P_0 = \frac{I_0 T_{\mathrm{af}} \alpha_f}{p}. \tag{6}$$

Note that the spectral dispersion of α_f and T_{af} implies the photon energy dependence of P_0 at fixed I_0.

B. Dynamics of the electron distribution f

We will suppose $\hbar\omega_p$ close to or lower than the interband transition threshold in gold $\hbar\omega_{\mathrm{ib}}$: the light pulse only induces intraband transitions within the sp conduction band where the number of electrons remains constant. At the L point of the Brillouin zone, $\hbar\omega_{\mathrm{ib}}$ value is 2.4 eV.[22]

At equilibrium, $f=f_0$ is a Fermi-Dirac distribution at room temperature T_0. Due to optical excitation, energy is instantaneously absorbed through intraband transitions, modifying f near the Fermi level. The system is thus out of equilibrium, i.e., it is impossible to ascribe a temperature to the electron gas. This corresponds to the athermal regime.[23] Internal electron energy redistribution takes place through electron-electron scattering and leads after a few hundreds of femtoseconds to the building up of a Fermi-Dirac distribution at temperature $T_e > T_0$. At the same time the electron gas also exchanges energy with the metal lattice through electron-phonon coupling until both are in a quasi-equilibrium state. This step takes place on a time scale of a few picoseconds. Finally, the energy relaxation toward the surrounding dielectric matrix should be taken into account. Nevertheless, we will focus in the following on the dynamics of f over time scales lower than 5 ps, i.e., for which the matrix has no significant influence on the electron dynamics.[24]

The nanoparticle size that will be considered is smaller than the optical penetration depth ($\sim$15 nm at 1.5 eV in gold). Therefore, we can assume a homogeneous excitation over each particle, ruling out any possibility of electron diffusion.[25]

Because of the nonequilibrium state of the electron gas in the first hundreds of femtosecond following the excitation, the dynamics of f has to be determined by solving the Boltzmann equation (BE). However, if the pulse duration is sufficiently large (about a few picoseconds), the internal thermalization of the electron gas is completed before the end of the pulse, f then being a Fermi-Dirac distribution at a defined electronic temperature T_e. The system is then described by an electron bath (at temperature T_e) interacting with the phonon bath of the metal lattice (at temperature T_l). Their time evolution can be determined by making use of the two-temperature model. We briefly describe these two theoretical approaches.

1. Boltzmann equation (BE)

The time evolution of the energy distribution function $f(E_{sp})$ for a sp electron of energy E_{sp}, which can be considered in gold as quasifree,[22] is governed by the BE,

$$\frac{\partial f(E_{sp})}{\partial t} = \left.\frac{\partial f(E_{sp})}{\partial t}\right|_{\mathrm{exc}} + \left.\frac{\partial f(E_{sp})}{\partial t}\right|_{\mathrm{e\text{-}e}} + \left.\frac{\partial f(E_{sp})}{\partial t}\right|_{\mathrm{e\text{-}ph}}. \tag{7}$$

The first term in the right-hand side describes the injection of energy by the optical pulse, while the two last terms

account, respectively, for the electron-electron (e-e) and electron-phonon (e-ph) scattering processes mentioned above. Several groups since the 1990s focused their attention on the resolution of this equation in the case of noble metals, from the pioneering work of Fann *et al.*[23] to the more rigorous treatment initiated by Sun *et al.*[26] and completed by Groeneveld *et al.*[27] and Del Fatti *et al.*[28] Let us now provide some details regarding each term of Eq. (7).

(i) Source term $\partial f/\partial t|_{\text{exc}}$. We use the approach developed in Ref. 28, which takes into account the finite duration τ_p of the pulse. $\partial f/\partial t|_{\text{exc}}$ can be written as the product of a time-dependent term $CP_{\text{abs}}(t)$ and an energy-dependent term $df_{\text{exc}}(E_{sp})$. The former represents the instantaneous power injected by metal volume unit as defined above [Eq. (4)]; C is a constant imposed by the total-energy conservation. $df_{\text{exc}}(E_{sp})$ accounts for the spectral range over which f_0 is modified by the laser pulse (i.e., $E_F \pm \hbar\omega_p$) and is the sum of a positive term and a negative one, corresponding, respectively, to the creation and the annihilation of an electron of energy E,

$$df_{\text{exc}}(E_{sp}) = f_0(E_{sp} - \hbar\omega_p)[1 - f_0(E_{sp})] - f_0(E_{sp})[1 - f_0(E_{sp} + \hbar\omega_p)]. \quad (8)$$

(ii) Electron-electron scattering term $\partial f/\partial t|_{\text{e-e}}$. The screened Coulombic scattering processes are responsible for both annihilation and creation of electrons of energy E_{sp}. In the weak perturbation limit, each excited electron scatters with an unperturbed one, i.e., interactions between two or more excited electrons are neglected.[29] We then use a relaxation-time approximation to describe the annihilation process:[25,29,30] the Landau theory of Fermi liquids gives a characteristic time $\tau_{\text{e-e}} = \tau_0 E_F^2/(E_{sp} - E_F)^2$.[31] This time diverges when $E_{sp} = E_F$, as a direct consequence of the Pauli exclusion principle. τ_0, which represents the lifetime that would have electrons without this exclusion principle, is taken as an adjustable parameter in our calculations. We determine its value by comparing our simulations with experimental measurements of the electron relaxation dynamics reported in Ref. 32. We then find $\tau_0 \approx 0.8$ fs, which is consistent with values found in the literature, ranging from 0.3 to 1.0 fs.[25,30,33] Electron creation processes are also treated in the relaxation-time approximation.[29,34] The only adjustable parameter needed to compute $\partial f/\partial t|_{\text{e-e}}$ is τ_0.

(iii) Electron-phonon scattering term $\partial f/\partial t|_{\text{e-ph}}$. Spontaneous emission, stimulated emission, and absorption of phonons contribute to this term. Contrary to the first case, the last two ones are characterized by scattering rates proportional to the number of available states in the phonon bath (described with a Bose-Einstein distribution at temperature T_l). We then separate $\partial f/\partial t|_{\text{e-ph}}$ into two contributions.[30] Each of them is treated in the relaxation-time approximation and depends on the energy-transfer rate $\dot{q}$ from the electron gas to the phonon bath.[25] The second one depends also on the number of phonons created by the excitation and on the mean phonon energy. A dimensionless factor S is introduced to adjust the relative weight of each process.[30]

2. Two-temperature model (TTM)

When the internal thermalization of the free-electron gas is completed, the common model used to describe the electron dynamics is the two-temperature model (TTM) developed by Kaganov *et al.*[35] The electron gas (the metal lattice) of the nanoparticle is considered as a bath at a temperature T_e (T_l) with specific heat C_e (C_l). C_e is proportional to T_e: $C_e = \gamma T_e$ with $\gamma = 66$ J m^{-3} K^{-2} for gold.[22] C_l follows the Dulong and Petit law (T_l being greater than the Debye temperature of gold $T_D = 170$ K) and has the value $C_l = 2.44 \times 10^{-6}$ J m^{-3} K^{-1}.[22] These two baths interact via the electron-phonon coupling, quantified by a constant $G = 3 \times 10^{16}$ W m^{-3} K^{-1},[36] and the temporal evolution of T_e and T_l is governed by two coupled equations,

$$C_e \frac{\partial T_e}{\partial t} = -G(T_e - T_l) + P_{\text{abs}}(t), \quad (9)$$

$$C_l \frac{\partial T_l}{\partial t} = G(T_e - T_l). \quad (10)$$

It should be noted that both the BE and the TTM are consistent since Eq. (9) can be obtained from Eq. (7) in the specific case where f is a Fermi-Dirac distribution at temperature T_e.[37]

C. Modification of the nanoparticle dielectric function

The optical properties of a material are described by its complex index $\tilde{n} = n + i\lambda\alpha/4\pi$ (n, α, and λ are the refractive index, absorption coefficient, and light wavelength in vacuum, respectively) or its dielectric function $\epsilon = \tilde{n}^2$. Following the optical pulse, the perturbation Δf of f close to the Fermi level modifies the spectrum of the interband transitions allowed between the d bands and the sp band. Consequently, it induces a modification $\Delta\epsilon^{\text{ib}}$ of their contribution to ϵ, as $\epsilon^{\text{ib}} = \epsilon^{\text{ib},0} + \Delta\epsilon^{\text{ib}}$. Note that the contribution of the interband transitions to the modification of ϵ is greatly predominant over the contribution of the intraband ones;[38] therefore the latter will be neglected in the following. To relate Δf to $\Delta\epsilon^{\text{ib}}$ we use the band-structure model of gold developed by Rosei *et al.*[39,40] In the visible spectral range under consideration here, the main contribution comes from the L point of the Brillouin zone.[40] For wave vectors close to this critical point, the band structure is described in the framework of the effective-mass approximation. It then reduces to a set of parabolic branches, the curvature of which is taken from Ref. 41. Using this model simplifies the calculation of the probability $J_{d\to p}(\hbar\omega)$ that a photon with energy $\hbar\omega$ induces a transition from the d bands to the sp band. The imaginary part of $\Delta\epsilon^{\text{ib}}$, $\Delta\epsilon_2^{\text{ib}}$, is then related to $J_{d\to p}(\hbar\omega)$ by using Lindhard's theory of the dielectric constant. This last step is done assuming that, near the critical point L, the modulus of the matrix element $|M^{d\to p}(\mathbf{k})|$ associated with a transition of wave vector $\mathbf{k}$ is independent of $\mathbf{k}$ (Ref. 40):

$$\epsilon_2^{\text{ib}}(\hbar\omega) \propto \frac{1}{\omega^2}|M^{d\to p}|^2 J_{d\to p}(\hbar\omega). \quad (11)$$

The corresponding real part of $\Delta\epsilon^{\text{ib}}$, noted $\Delta\epsilon_1^{\text{ib}}$, is finally obtained through the Kramers-Kronig relation, using the numerical method proposed by Castro and Nabet,[42] which is based on a Hilbert transform. We have verified the validity of this approach by processing the experimental data of ϵ for gold.[43]

Experimental setups such as z-scan or DFWM in their conventional configuration are frequently used to measure third-order susceptibilities of materials. In this kind of experiments the pulse plays the role of both the excitation and the probe. As to describe such an experimental situation, we use the approach we proposed in Ref. 24, defining the effective mean change of the interband dielectric function $\overline{\Delta\epsilon^{\mathrm{ib}}}$ experienced by the detected probe pulse,

$$\overline{\Delta\epsilon^{\mathrm{ib}}}(\omega) = \frac{\int_{-\infty}^{+\infty} \Delta\epsilon^{\mathrm{ib}}(\omega,t) P_{\mathrm{abs}}(t) dt}{\int_{-\infty}^{+\infty} P_{\mathrm{abs}}(t) dt}. \quad (12)$$

It is then straightforward to extract the value of the effective mean change of both the refractive index ($\overline{\Delta n}$) and the absorption coefficient ($\overline{\Delta\alpha}$), as will be done later. Note that some experimental works have been focused on the time evolution of the nonlinear response, for which Eq. (12) would have no meaning. For instance, Liao *et al.*[44] extended the usual DFWM, where the three incident beams arrive simultaneously onto the sample, to a time-resolved scheme, by introducing an adjustable delay for the third pulse. Here we deal only with non-time-resolved schemes.

D. Definition and expression of $\chi_{\mathrm{he}}^{(3)}$

Equation (1), which concerns the optical Kerr effect, can be written as a function of the incident wave intensity $I(\omega) = 2cn_{0m}(\omega)\epsilon_0|E(\omega)|^2$ (monochromatic plane wave with circular frequency ω). n_{0m} and c are, respectively, the material refractive index and the speed of light in vacuum. From Eq. (1), we then obtain the expression relating $\chi^{(3)}(\omega)$ to $\Delta\epsilon(\omega)$:

$$\chi^{(3)}(\omega) = \frac{2cn_{0m}(\omega)\epsilon_0}{3I(\omega)} \Delta\epsilon(\omega). \quad (13)$$

The way we define the hot electron contribution to the third-order susceptibility is analogous to the one used for the optical Kerr effect, replacing $\chi^{(3)}$ and $\Delta\epsilon$ with $\chi_{\mathrm{he}}^{(3)}$ and $\overline{\Delta\epsilon^{\mathrm{ib}}}$, respectively,

$$\chi_{\mathrm{he}}^{(3)}(\omega) = \frac{2cn_{0m}(\omega)\epsilon_0}{3I_0(\omega)} \overline{\Delta\epsilon^{\mathrm{ib}}}(\omega), \quad (14)$$

where n_{0m} is now the refractive index of gold, I_0 refers to the temporal maximum of the incident pulse intensity, and $\overline{\Delta\epsilon^{\mathrm{ib}}}$ is calculated through Eq. (12). $\chi_{\mathrm{he}}^{(3)}$ is then linked with $\overline{\Delta n}$ and $\overline{\Delta\alpha}$ by

$$\chi_{\mathrm{he}}^{(3)} = \frac{4cn_{0m}}{3I_0} \tilde{n} \left(\overline{\Delta n} + i \frac{\lambda}{4\pi} \overline{\Delta\alpha} \right). \quad (15)$$

III. PULSE WIDTH, SPECTRAL, AND INTENSITY DEPENDENCE OF $\chi_{\mathrm{he}}^{(3)}$

A. Representative virtual samples

In order to study the influence of the material linear optical response on the hot electron contribution to $\chi_m^{(3)}$, we will apply the theoretical approach developed for $\chi_{\mathrm{he}}^{(3)}$ to two representative virtual nanocomposite thin films, S_1 and S_8. They consist of spherical gold nanoparticles randomly dispersed in a silica matrix with metal volume fractions $p=1\%$ and 8%, respectively.

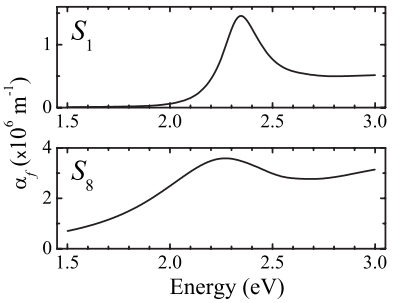

FIG. 1. Linear absorption coefficient of samples S_1 (top) and S_8 (bottom) as a function of photon energy.

S_1 is a model sample where nanoparticles remain small as compared with the light wavelength but are large enough (typically with a diameter greater than 10 nm) to avoid finite-size effects which could affect the characteristics of the SPR.[1] The linear optical properties of such a heterogeneous medium can be described in the framework of an effective-medium theory. We have used the Maxwell-Garnett one which is well suited in this specific case where electromagnetic interactions between nanoparticles are negligible.[45] Dielectric functions of gold and silica are taken as those of the bulk phases.[43] We obtain the spectrum of the linear absorption coefficient α_f of S_1, which is displayed in Fig. 1(a). As can be seen, the SPR band peaks at 2.35 eV, while interbands transitions are responsible for the absorption in the UV part of the spectrum.

The second sample S_8 has an optical response similar to the one of a thin-film elaborated in our laboratory by the radio-frequency sputtering technique.[46] The diameter of the nanoparticles is about a few nanometers. Finite-size effects are then no longer negligible, implying a modification of the SPR characteristics (spectral position, amplitude, and width). Avoiding further details which can be found in Ref. 47, let us mention that for S_8 we partially account for such effects by simply considering the electron mean-free-path limitation due to confinement.[1]

Let us stress that considering highly concentrated nanocomposite media (i.e., including the influence of electromagnetic interactions between neighboring nanoparticles) would only change the value of the effective absorption coefficient α_f, the local-field factor f, and the approach leading to the effective-medium third-order susceptibility [Eq. (2)]. As in the present paper we focus on the calculation of the nanoparticle intrinsic susceptibility, the only parameter involved in this calculation which would be sensitive to the medium morphology is α_f (exactly as what will demonstrated by looking at the differences between samples S_1 and S_8). Our approach for calculating $\chi_{\mathrm{he}}^{(3)}$ is then fully applicable for higher metal volume fractions as soon as the medium absorption coefficient is known.

Figure 1 displays the absorption coefficient of S_1 and S_8. The SPR band quenching and broadening with reducing particle size, accounted for by this phenomenological approach, can be observed in the comparison of the two plots.

TABLE I. Selected results for $\chi_m^{(3)}$ of gold nanoparticles determined, either experimentally or by calculation. I_0 remains lower than the critical value defined in Sec. III D. Note that the calculated values of $\chi_m^{(3)}$ correspond to the hot electron contribution only.

τ_p	$\hbar\omega$ (eV)	Method	$\lvert\chi_{he}^{(3)}\rvert$ (esu)	ϕ (deg)	Reference
50 fs	2.20	BE	3.4×10^{-9}	158	This work
110 fs	2.21	Z-scan	9.0×10^{-10}	191	48
200 fs	2.33	DFWM	3.4×10^{-9}	NA	44
250 fs	2.33	BE	3.0×10^{-9}	93	This work
2 ps	2.39	TTM	2.9×10^{-7}	84	This work
5 ps	2.33	OPC[a]	5×10^{-8}	80	9
5 ps	2.05–2.21	DFWM	2.5×10^{-8}	N.A.	49
5 ps	2.33	Calc.	1.1×10^{-7}	~90	9

[a]Optical phase conjugation.

B. Pulse duration dependence of the nonlinear optical response

In this subsection, we will study the influence of the pulse duration τ_p, within the range of 50 fs–5 ps, on the complex nonlinear response. For this, the time evolution of f will be evaluated, either by the TTM or by the BE, as exposed in Sec. II.

Calculations will be presented for optical pulses with photon energy $\hbar\omega=1.5$ eV. The study of the pulse width influence on the nonlinear optical response is meaningful only if it is performed at a constant value of the total energy injected per metal volume unit, E_{abs}. E_{abs} is equal to $\int_{-\infty}^{+\infty}P_{\text{abs}}(t)dt$, i.e., proportional to the product $P_0\tau_p$. We will then tune P_0 so as to keep the product $P_0\tau_p$ constant. Moreover, calculations are carried out in the weak perturbation regime, which allows us to apply the method exposed in Sec. II for solving the BE. To quantify the magnitude of this perturbation, we evaluate the density of conduction electrons out of equilibrium at the maximum of the excitation, $n_e=\int_{E_F}^{+\infty}\rho(E_{sp})[f(E_{sp})-f_0(E_{sp})]dE_{sp}$. In this expression, ρ is the density of states in the conduction band while f and f_0 have the same meaning as in Sec. II. Then, we compare n_e to the total density of conduction electrons in gold $n_{e,0}$, the value of which is $n_{e,0}=5.9\times10^{28}$ m^{-3}.[22] The excitation parameters are chosen as to match the usual laser characteristics in a z-scan experiment (~50 μm waist radius and 50 nJ pulse energy): $\tau_p=250$ fs and $P_0=10^{20}$ W m^{-3}. With these values, $n_e=3.5\times10^{25}$ m^{-3} and $n_e/n_{e,0}\sim10^{-3}$, which confirms the validity of the weak perturbation hypothesis. If we fix the limit at $n_e/n_{e,0}=1\%$, then the maximum value of P_0 ensuring the validity of our approach is about 10^{21} W m^{-3} for 250 fs pulses. To sum up, we will take $P_0=10^{20}$ W m^{-3} for $\tau_p=250$ fs and then adapt these values to maintain the product $P_0\tau_p$ constant.

The pulse width dependence of the hot electron contribution to the intrinsic gold nanoparticle third-order nonlinear response will be analyzed through the relative mean variation over the pulse duration of both the refractive index $(\overline{\Delta n/n_0})$ and the absorption coefficient $(\overline{\Delta\alpha/\alpha_0})$, the expressions of which are obtained from Eq. (12). n_0 and α_0 are, respectively, the values of n and α for gold at 1.5 eV at equilibrium: $n_0=0.189$ and $\alpha_0=1.25\times10^8$ m^{-1}.[43] The choice of Δn and $\Delta\alpha$, rather than $\chi_{\text{he}}^{(3)}$, for highlighting the influence of pulse width on the nonlinear response is driven by the fact that we want to keep the total pulse energy constant, which imposes the variation in the intensity with τ_p. The further calculation of $\chi_{\text{he}}^{(3)}$ then depends on the knowledge of the intensity value [see Eq. (15)], which is not an intrinsic parameter but an experimental one. Once I_0 is known, $\chi_{\text{he}}^{(3)}$ can nevertheless be determined from Δn and $\Delta\alpha$. Examples are provided in Table I.

One can notice that reducing the pulse duration to a few hundreds of femtoseconds leads to a drastic decrease in the value of $\lvert\chi_{\text{he}}^{(3)}\rvert$. This is both experimentally measured and calculated by our approach, and has been already underlined elsewhere (see Table 1 of Ref. 50). Let us now go deeper into the pulse width influence on the hot electron contribution to the nonlinear response. The evolution of $\overline{\Delta n/n_0}$ and $\overline{\Delta\alpha/\alpha_0}$ with τ_p is displayed in Figs. 2(a) and 2(b).

A first glance at Fig. 2 reveals that whatever the model used and for a fixed total energy absorbed by the nanoparticle, both nonlinear refraction and absorption induced by hot electrons tend to zero as the pulse width increases. Moreover, for short pulses, i.e., with τ_p lower than about 1 ps, there is a great discrepancy between the TTM and the BE approaches, for both the refractive [Fig. 2(a)] and the absorptive [Fig. 2(b)] parts of the optical response. This difference is due to the noninstantaneous thermalization of the electron gas, which is taken into account in the BE approach only. This thermalization originates from e-e scattering, to which is associated a characteristic time on the order of a few hundreds of femtoseconds (450 fs in bulk gold).[51] Let us recall that in non-time-resolved experimental setups such as conventional z-scan, the optical pulse plays at the same time the role of both pump and probe. Then, for pulses with τ_p of the order of a few picoseconds, the internal thermalization is almost achieved before the end of the probe pulse; consequently, the modification of the optical properties is less sensitive to the athermal regime than for shorter pulses. This explains that the differences between the values of $\overline{\Delta n/n_0}$ and $\overline{\Delta\alpha/\alpha_0}$ predicted by the TTM and the BE decrease with increasing τ_p.

This study reveals that for pulses with a duration τ_p of a few hundreds of femtoseconds the understanding of the

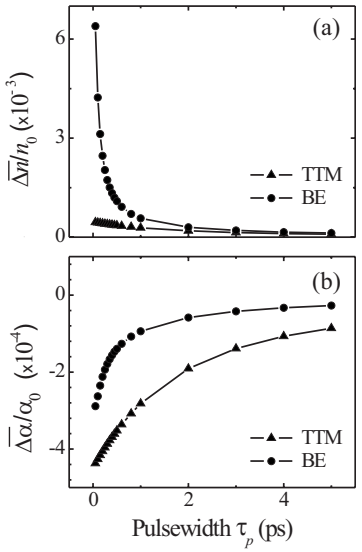

FIG. 2. Effective modification over the pulse duration of (a) the refractive index and (b) the absorption coefficient of gold as a function of the pulse width for $\hbar\omega=1.5$ eV. Circles and triangles correspond to results obtained, respectively, in the BE and the TTM approaches with $P_0\tau_p=25$ MJ m^{-3}.

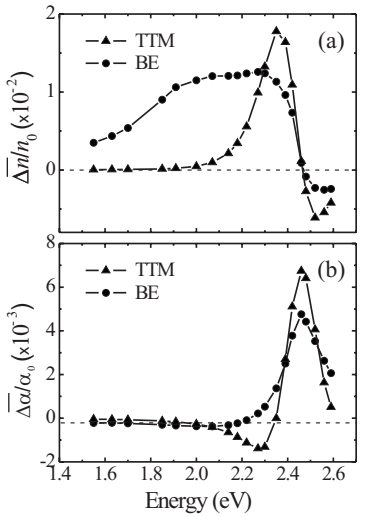

FIG. 3. Effective relative modification over the pulse duration of (a) the refractive index and (b) the absorption coefficient of gold as a function of the photon energy. Results are obtained by solving BE with $\tau_p=250$ fs and $P_0=10^{20}$ W m^{-3} (circles) and TTM with $\tau_p=2$ ps and $P_0=1.25\times10^{19}$ W m^{-3} (triangles).

third-order nonlinear optical properties of metal nanoparticles requires to take into account the noninstantaneous thermalization of the conduction-electron gas. The TTM is thus wholly inappropriate in this ultrashort pulse regime.

C. Spectral dependence of the nonlinear optical response

This part aims at investigating the spectral dependence of $\chi_{\mathrm{he}}^{(3)}$ and the consequences of the athermal regime on this dispersion. We choose as in Sec. III B a constant pulse energy, with a pulse duration $\tau_p=250$ fs and an excitation magnitude $P_0=10^{20}$ W m^{-3}, for the BE approach, and $\tau_p=2$ ps and $P_0=1.25\times10^{19}$ W m^{-3} for the TTM.

Having a close look at Eq. (14), which formally defines the hot electron contribution to $\chi_m^{(3)}$, it appears that the spectral dispersion of $\chi_{\mathrm{he}}^{(3)}$ may stem from either $\overline{\Delta\epsilon^{\mathrm{ib}}}(\omega)$, that is to say from the *nonlinear* optical response intrinsic to gold, or from $I_0(\omega)/n_{0m}(\omega)$, which comes from the spectral dependence of the *linear* optical properties of the material. In the following, we will thus turn successively our attention onto these two contributions.

We first consider the dispersion of $\chi_{\mathrm{he}}^{(3)}$ arising from the *intrinsic* nonlinear response of gold, through $\overline{\Delta\epsilon^{\mathrm{ib}}}$, which is split into a refractive part and an absorptive one as in Eq. (15). These two contributions will be characterized by the relative variations in the refractive index, $\overline{\Delta n}/n_0$, and the absorption coefficient, $\overline{\Delta\alpha}/\alpha_0$. On Fig. 3(a) [Fig. 3(b)] is displayed the spectrum of $\overline{\Delta n}/n_0$ ($\overline{\Delta\alpha}/\alpha_0$), using either the BE (circles) or the TTM (triangles) approach.

It is worth mentioning that, whereas the magnitude of the complex nonlinear response, as given by the TTM, varies with the pulse duration, its spectral profile is almost independent of τ_p. In the precise aim of underlining the influence of the athermal regime on the hot electron contribution spectral dependence, it is then possible to compare the curves obtained with the BE and TTM approaches on Fig. 3.

Let us first examine the refractive part $\overline{\Delta n}/n_0$. The spectral dependence of its sign is the same whether the athermal regime is considered or not: it is positive at low energies and it becomes negative around 2.45 eV, i.e., close to the interband transition threshold. However, the magnitude of $\overline{\Delta n}/n_0$ and the spectral range on which it differs from zero is strongly dependent on the theoretical approach used. These differences stem from the way the perturbation is taken into account in each model. Concerning the BE approach, the optical pulse, in its role of pump, induces a modification of the electron distribution f on a wide spectral range, between $E_F-\hbar\omega_p$ and $E_F+\hbar\omega_p$ (cf. Sec. II B 1). The same optical pulse, now in its role of probe, can therefore be sensitive to this modification even if the photon energy differs significantly from $\hbar\omega_{\mathrm{ib}}$.

The magnitude of the absorptive part $\overline{\Delta\alpha}/\alpha_0$ is also greatly overestimated when the athermal regime is ignored. Furthermore, the sign of $\overline{\Delta\alpha}/\alpha_0$ given by the TTM can be opposite to the one predicted by the BE in certain spectral domain. Let us compare these results with the experimental ones presented in Ref. 26. The authors of this reference reported measurements of the modification of both the reflectivity and the transmissivity (respectively, $\Delta R/R$ and $\Delta T/T$ in their paper) of a thin gold film, following a subpicosecond optical excitation. They showed that for photon energies around 2.35 and 2.70 eV the athermal regime gives birth to a positive $\Delta R/R$ in the first hundreds of femtoseconds, while as soon as the electron gas is thermalized $\Delta R/R$ becomes positive. They found a similar behavior for $\Delta T/T$. In the weak perturbation regime, both $\Delta R/R$ and $\Delta T/T$ can be expressed as linear combinations of $\overline{\Delta n}/n_0$ and $\overline{\Delta\alpha}/\alpha_0$. It is therefore consistent to find that for some photon energies the values of $\overline{\Delta\alpha}/\alpha_0$ (and/or $\overline{\Delta n}/n_0$) calculated by using the BE exhibited a sign opposite to the one obtained with the TTM.

The discussion above concerns contribution to the dispersion of $\chi_{\mathrm{he}}^{(3)}$ originating from the intrinsic nonlinear optical

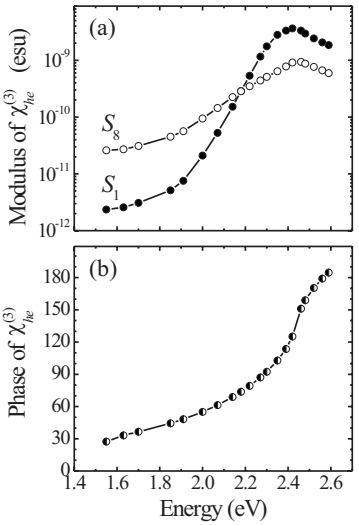

FIG. 4. (a) Modulus (in esu) and (b) phase (in degrees) of $\chi^{(3)}_{\mathrm{he}}$ as a function of the photon energy for samples S_1 (full circles) and S_8 (empty circles). These results are obtained in the BE approach with $\tau_p=250$ fs and $P_0=10^{20}$ W m^{-3}.

response of gold. However, as was mentioned earlier, this is not the only contribution since the influence of the linear optical properties of the composite medium has to be taken into account. Indeed, for a given P_0 value, $\chi^{(3)}_{\mathrm{he}}$ varies as α_f through I_0/n_{0m} [see Eqs. (14) and (6)]. We will now highlight this effect by studying the dispersion of $\chi^{(3)}_{\mathrm{he}}$ for both samples presented in Sec. III A. We will adopt the notation $\chi^{(3)}_{\mathrm{he}}=|\chi^{(3)}_{\mathrm{he}}|e^{i\phi}$ since most of experiments give access to $|\chi^{(3)}_{\mathrm{he}}|$.

In Fig. 4(a) the modulus of $\chi^{(3)}_{\mathrm{he}}$ is presented as a function of photon energy, for samples S_1 (full circles) and S_8 (empty circles), determined by using the BE approach. The comparison of these curves underlines the strong influence of the linear optical response on the dispersion of $|\chi^{(3)}_{\mathrm{he}}|$: over the spectral range considered, it evolves within less than 2 orders of magnitude for S_8 against 3 for S_1. This has of course to be linked with the relative variations in the SPR absorption band as displayed in Fig. 1. The contribution of the dispersion of α_f is then crucial when experimental measurements of $|\chi^{(3)}_{\mathrm{he}}|$ are compared to theoretical predictions. The huge enhancement of $|\chi^{(3)}_{\mathrm{he}}|$ around the SPR is not the consequence of any nonlinear effect but is only due to a stronger linear absorption. It is therefore more relevant to use the peak power P_0 absorbed per metal volume unit rather than the peak intensity I_0 of the incident laser beam to characterize the optical excitation in an experimental study.

The situation is totally different concerning the phase of $\chi^{(3)}_{\mathrm{he}}$, ϕ. Indeed, a glance at Eq. (14) reveals that the only quantity having *a priori* an imaginary part is $\overline{\Delta\epsilon^{\mathrm{ib}}}$. Therefore, the phase of $\chi^{(3)}_{\mathrm{he}}$ is the same as the one of $\overline{\Delta\epsilon^{\mathrm{ib}}}$ and is completely independent of the linear-response of the sample. This is illustrated on Fig. 4(b) where the curves for S_1 and S_8 are perfectly identical. As can be seen, ϕ largely evolves over the visible domain, but remains within the range $0°-180°$. This means that the imaginary part of $\chi^{(3)}_{\mathrm{he}}$ is positive (this is no more true in the UV domain, from ~2.6 eV). Moreover, $\chi^{(3)}_{\mathrm{he}}$ is mainly imaginary ($\phi\sim 90°$) and its phase dispersion $\partial\phi/\partial\omega$ is maximum around $\hbar\omega\sim 2.4$ eV, close to the interband transition threshold.

We will now compare our theoretical results to measurements obtained by Liao *et al.*[44] on Au:SiO_2 thin films with $p=8\%$ (see Table I). These were realized with a DFWM setup with 200 fs laser pulses at 2.33 eV. The physical quantity deduced from these measurements is the effective third-order nonlinear susceptibility $\chi^{(3)}_{\mathrm{eff}}$ [cf. Eq. (2)]. As metal concentration remains sufficiently low to neglect electromagnetic interactions between nanoparticles and as the latter are small enough to consider the internal electric field as homogeneous, f_l roughly follows Eq. (3). It is then possible to deduce the value of the third-order nonlinear susceptibility of gold nanoparticles, $\chi^{(3)}_m$, from Eq. (2). The authors found $|\chi^{(3)}_m|=3.4\times 10^{-9}$ esu at 2.33 eV. Our calculation at this photon energy gives $|\chi^{(3)}_{\mathrm{he}}|=3\times 10^{-9}$ esu [cf. Fig. 4(a)]. This result confirms what we inferred in Sec. I, which is to say the dominant weight of the hot electron contribution to $|\chi^{(3)}_m|$ as compared with that of intraband and interband contributions in the vicinity of the interband transition threshold. This conclusion is the same as the one exposed by Hache *et al.*[9] for 5 ps pulses. All these results are summarized in Table I for easier comparison. Note that Liao *et al.*[44] found values of $|\chi^{(3)}_m|$ much higher for 35 ps pulses than for 200 fs ones. This trend was also revealed by many other investigations reported in the literature (see Table 1 of Ref. 50). This stems from the dominant contribution of the thermo-optical response when using long pulses.[47,52]

D. Intensity dependence of $\chi^{(3)}_{\mathrm{he}}$

We will now show that above a certain intensity onset, which varies with photon energy, the value of $\chi^{(3)}_{\mathrm{he}}$ can be no longer independent of I_0. It is worth mentioning that such a study cannot be carried out for subpicosecond pulses within our present approach. Indeed, as stated before, the presence of the athermal regime requires the use of the BE, which is limited in intensity by the weak perturbation hypothesis in our model.

We consider sample S_1 excited by a 2 ps pulse. This pulse width allows us to carry out calculations in the framework of the TTM model, with different photon energies and over a wide laser intensity range (from $\sim 10^3$ to $\sim 10^{10}$ W cm^{-2}). The modulus and phase of $\chi^{(3)}_{\mathrm{he}}$ are displayed, respectively, in Figs. 5(a) and 5(b) as a function of I_0.

The same trend as in Fig. 4 is of course exhibited by Fig. 5: $|\chi^{(3)}_{\mathrm{he}}|$ and ϕ experience a strong dispersion. This result is a first confirmation that the quantitative predictions of Hache *et al.*[9] cannot be extended to photon energies different from ~2.33 eV, which is the one considered in Ref. 9. Furthermore, remaining at low I_0 (typically less than 10^6 W cm^{-2}), the model we have developed above for the calculation of $\chi^{(3)}_{\mathrm{he}}$ gives orders of magnitude for $|\chi^{(3)}_{\mathrm{he}}|$ and ϕ similar to those reported in Ref. 9 (see Table I). Besides, Hache *et al.*[9] first found that $\chi^{(3)}_{\mathrm{he}}$ is mainly imaginary at 2.33 eV, as we predict at 2.39 eV where $\phi\sim 90°$, and second they obtained $|\chi^{(3)}_{\mathrm{he}}|\sim 1.1\times 10^{-7}$ esu while our model gives $|\chi^{(3)}_{\mathrm{he}}|\sim 2.9\times 10^{-7}$ esu at 2.39 eV. The small difference between these two values can come from the slight mismatch of either the photon energies or the pulse widths between Ref. 9 and the present calculations.

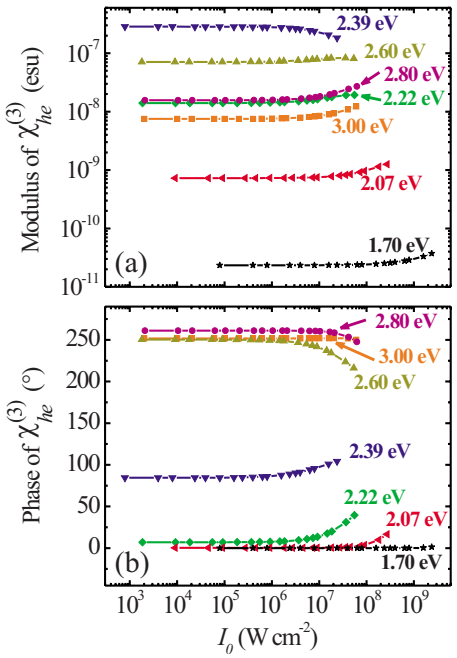

FIG. 5. (Color online) (a) Modulus (in esu) and (b) phase (in degrees) of $\chi^{(3)}_{\mathrm{he}}$ for the sample S_1 as a function of the incident intensity I_0 and for different photon energies. These results are obtained by the TTM approach with τ_p=2 ps.

Finally, when the intensity of the incident laser beam exceeds a critical value, both $|\chi^{(3)}_{\mathrm{he}}|$ and ϕ become intensity dependent. This critical value in terms of P_0, $P_{0,\max}$, depends on pulse duration (for τ_p=2 ps, $P_{0,\max}=4\times10^{18}$ W m^{-3}): $P_{0,\max}$ decreases as pulse width increases. Indeed, the relevant criterion here is the total energy deposited at the end of the pulse, E_{abs}. Expressed in terms of intensity, the critical value $I_{0,\max}$ depends additionally on the material linear optical properties and then on photon energy via the dispersion of the latter [see Eq. (5)]. Hence, for instance, the value of $I_{0,\max}$ with 2 ps pulses is $\sim10^6$ W cm^{-2} at 2.39 eV or 10^8 W cm^{-2} at 1.70 eV. Let us stress that, nowadays, picosecond lasers commonly used to measure nonlinear susceptibilities deliver pulses with maximum peak intensity from $\sim10^5$ to $\sim10^9$ W cm^{-2}. This last value is well over the critical intensity from which $\chi^{(3)}_{\mathrm{he}}$ is no longer constant in Fig. 5. This means that in this high excitation regime, which can be easily reached in experiments, the hot electron contribution to the nonlinear optical properties of nanocomposite materials is no longer a pure third-order nonlinear effect. The predictions of Hache *et al.*,[9] which were obtained assuming a low excitation regime, have then to be considered with care when the validity of this hypothesis breaks.

IV. CONCLUSION

We have presented a theoretical approach for evaluating the hot electron contribution to the intrinsic third-order nonlinear susceptibility of gold nanoparticles excited by subpicosecond or picosecond laser pulses. This issue had been addressed in the pioneering work of Hache *et al.*[9] where calculations were carried out with restricted conditions regarding photon energy (close to both $\hbar\omega_{\mathrm{ib}}$ and the SPR energy), pulse duration (5 ps), and intensity (weak perturbation regime). Computing the electron dynamics in the framework of both the Boltzmann equation and the two-temperature model for different pulse durations, we have shown the growing importance of the athermal regime on the magnitude and the dispersion of the nonlinear optical response as the pulse duration falls below approximately 1 ps. We have then evaluated $\chi^{(3)}_{\mathrm{he}}$ for two different virtual samples. Contrary to the phase of $\chi^{(3)}_{\mathrm{he}}$, its modulus has been shown to strongly depend on the linear optical properties of the material. Comparing our calculations with experimental results of Liao *et al.*,[44] we have shown that the hot electron contribution is the predominant one to $|\chi^{(3)}_m|$ in the ultrashort pulse excitation regime. This also argues with the conclusion of Hache *et al.*[9] obtained for 5 ps pulses. Finally, we have shown in the case of 2 ps pulses that our predictions are consistent with those of Ref. 9. However, $\chi^{(3)}_{\mathrm{he}}$ becomes intensity dependent when the intensity of the incident beam exceeds a critical value which depends on both the photon energy and the material linear absorption. This onset can even be lower than the common intensities used in experiments. Therefore, in the high excitation regime, the hot electron contribution does no longer amounts to a pure third-order nonlinear optical effect.

Due to the importance of the athermal regime, the TTM approach is inadequate for subpicosecond pulses. On the contrary, the method based on the BE resolution is well suited whatever the pulse width. The approach proposed in this paper, which presents the advantage of being quite easily carried out from a computational point of view, is nevertheless restricted to the weak excitation regime (from P_0=0 to $\sim10^{21}$ W m^{-3} for 250 fs pulses, corresponding to I_0=0 to $\sim$2.5 GW cm^{-2} for sample S_8 at SPR). To overcome this limitation, one would rather adopt a more complex model to account in the BE for interactions between two or more excited electrons, which have been disregarded here.[28]

Let us also stress that, as soon as the pulse duration reaches about 5 ps, the thermal influence of the particle environment cannot be neglected anymore.[24] We have proposed different theoretical approaches to account for such an effect.[24,52,53] For even longer pulses, the thermo-optical response of metal particles may also play a significant role in their nonlinear optical properties.[54,55]

A more systematic experimental study of the spectral and intensity dependences of $\chi^{(3)}_{\mathrm{he}}$ in gold nanoparticles should be interesting to allow detailed comparison with the predictions of our model. The experiments should be performed on samples with a low gold volume fraction in order to easily relate the effective third-order nonlinear susceptibility of the thin film to the metal intrinsic one. Let us also note that even if we have focused here on the case of gold, this model would be easily extended to the case of silver or copper.

ACKNOWLEDGMENTS

The authors thank the French Agence Nationale de la Recherche for its financial support (program ANR/PNANO 2006, project EThNA).

*bruno.palpant@upmc.fr

[1] U. Kreibig and M. Vollmer, *Optical Properties of Metal Clusters* (Springer-Verlag, Berlin, 1995).

[2] K. Awazu, M. Fujimaki, C. Rockstuhl, J. Tominaga, H. Murakami, Y. Ohki, N. Yoshida, and T. Watanabe, J. Am. Chem. Soc. **130**, 1676 (2008).

[3] C. Tominaga, J. adn Mihalcea, D. Büchel, H. Fukuda, T. Nakano, N. Atoda, H. Fuji, and T. Kikukawa, Appl. Phys. Lett. **78**, 2417 (2001).

[4] H. Ditlbacher, J. R. Krenn, B. Lamprecht, A. Leitner, and F. R. Aussenegg, Opt. Lett. **25**, 563 (2000).

[5] L. R. Hirsch, R. J. Stafford, J. A. Bankson, S. R. Sershen, B. Rivera, R. E. Price, J. D. Hazle, N. J. Halas, and J. L. West, Proc. Natl. Acad. Sci. U.S.A. **100**, 13549 (2003).

[6] K. Sokolov, M. Follen, J. Aaron, I. Pavlova, A. Malpica, R. Lotan, and R. Richards-Kortum, Cancer Res. **63**, 1999 (2003).

[7] A. Iwakoshi, T. Nanke, and T. Kobayashi, Gold Bull. **38**, 107 (2005).

[8] F. Hache, D. Ricard, and C. Flytzanis, J. Opt. Soc. Am. B **3**, 1647 (1986).

[9] F. Hache, D. Ricard, C. Flytzanis, and U. Kreibig, Appl. Phys. A: Solids Surf. **47**, 347 (1988).

[10] D. Compton, L. Cornish, and E. van der Lingen, Gold Bull. **36**, 10 (2003).

[11] D. Compton, L. Cornish, and E. van der Lingen, Gold Bull. **36**, 51 (2003).

[12] D. Stroud and P. M. Hui, Phys. Rev. B **37**, 8719 (1988).

[13] D. Stroud and V. E. Wood, J. Opt. Soc. Am. B **6**, 778 (1989).

[14] H. Ma, R. Xiao, and P. Sheng, J. Opt. Soc. Am. B **15**, 1022 (1998).

[15] V. M. Shalaev, *Nonlinear Optics of Random Media: Fractal Composites and Metal-Dielectric Films* (Springer, Berlin, 2000).

[16] R. W. Boyd, *Nonlinear Optics* (Academic, San Diego, 1992).

[17] D. D. Smith, Y. Yoon, R. W. Boyd, J. K. Campbell, L. A. Baker, R. M. Crooks, and M. George, J. Appl. Phys. **86**, 6200 (1999).

[18] B. Buchalter and G. R. Meredith, Appl. Opt. **21**, 3221 (1982).

[19] S. Santran, L. Canioni, L. Sarger, T. Cardinal, and E. Fargin, J. Opt. Soc. Am. B **21**, 2180 (2004).

[20] D. Ricard, P. Roussignol, and C. Flytzanis, Opt. Lett. **10**, 511 (1985).

[21] G. L. Eesley, Phys. Rev. Lett. **51**, 2140 (1983).

[22] N. W. Ashcroft and N. D. Mermin, *Solid State Physics* (Holt Saunders, Philadelphia, 1976).

[23] W. S. Fann, R. Storz, H. W. K. Tom, and J. Bokor, Phys. Rev. B **46**, 13592 (1992).

[24] M. Rashidi-Huyeh and B. Palpant, J. Appl. Phys. **96**, 4475 (2004).

[25] V. E. Gusev and O. B. Wright, Phys. Rev. B **57**, 2878 (1998).

[26] C.-K. Sun, F. Vallée, L. H. Acioli, E. P. Ippen, and J. G. Fujimoto, Phys. Rev. B **50**, 15337 (1994).

[27] R. H. M. Groeneveld, R. Sprik, and A. Lagendijk, Phys. Rev. B **51**, 11433 (1995).

[28] N. Del Fatti, C. Voisin, M. Achermann, S. Tzortzakis, D. Christofilos, and F. Vallée, Phys. Rev. B **61**, 16956 (2000).

[29] G. Tas and H. J. Maris, Phys. Rev. B **49**, 15046 (1994).

[30] C. Suárez, W. E. Bron, and T. Juhasz, Phys. Rev. Lett. **75**, 4536 (1995).

[31] D. Pines and P. Nozières, *Normal Fermi Liquids*, The Theory of Quantum Liquids Vol. I (Benjamin, New York, 1966).

[32] C.-K. Sun, F. Vallée, L. Acioli, E. P. Ippen, and J. G. Fujimoto, Phys. Rev. B **48**, 12365 (1993).

[33] H. Ehrenreich and M. H. Cohen, Phys. Rev. **115**, 786 (1959).

[34] R. H. Ritchie, J. Appl. Phys. **37**, 2276 (1966).

[35] M. I. Kaganov, I. M. Lifshitz, and L. V. Tanatarov, Sov. Phys. JETP **4**, 173 (1957).

[36] Y. Hamanaka, J. Kuwabata, I. Tanahashi, S. Omi, and A. Nakamura, Phys. Rev. B **63**, 104302 (2001).

[37] P. B. Allen, Phys. Rev. Lett. **59**, 1460 (1987).

[38] J.-Y. Bigot, V. Halté, J.-C. Merle, and A. Daunois, Chem. Phys. **251**, 181 (2000).

[39] R. Rosei, Phys. Rev. B **10**, 474 (1974).

[40] M. Guerrisi, R. Rosei, and P. Winsemius, Phys. Rev. B **12**, 557 (1975).

[41] M. Perner, Ph.D. thesis, Ludwig-Maximilians-Universität München, 1999.

[42] F. Castro and B. Nabet, J. Franklin Inst. **336**, 53 (1999).

[43] E. D. Palik, *Handbook of Optical Constants of Solids* (Academic, New York, 1985).

[44] H. B. Liao, R. F. Xiao, J. S. Fu, H. Wang, K. S. Wong, and G. K. L. Wong, Opt. Lett. **23**, 388 (1998).

[45] J. C. Maxwell Garnett, Philos. Trans. R. Soc. London, Ser. A **203**, 385 (1904).

[46] N. Pinçon-Roetzinger, D. Prot, B. Palpant, E. Charron, and S. Debrus, Mater. Sci. Eng., C **19**, 51 (2002).

[47] B. Palpant, M. Rashidi-Huyeh, B. Gallas, S. Chenot, and S. Fisson, Appl. Phys. Lett. **90**, 223105 (2007).

[48] B. Palpant, D. Prot, A.-S. Mouketou-Missono, M. Rashidi-Huyeh, C. Sella, and S. Debrus, Proc. SPIE **5221**, 14 (2003).

[49] K. Puech, W. Blau, A. Grund, C. Bubeck, and G. Cardenas, Opt. Lett. **20**, 1613 (1995).

[50] B. Palpant, in *Nonlinear Optical Properties of Matter: From Molecules to Condensed Phases*, Challenges and Advances in Computational Chemistry and Physics Vol. 1, edited by M. G. Papadopoulos, J. Leszczynski, and A. J. Sadlej (Springer, New York, 2006), pp. 461–508.

[51] J. Lermé, G. Celep, M. Broyer, E. Cottancin, M. Pellarin, A. Arbouet, D. Christofilos, C. Guillon, P. Langot, N. Del Fatti, and F. Vallée, Eur. Phys. J. D **34**, 199 (2005).

[52] B. Palpant, Y. Guillet, M. Rashidi-Huyeh, and D. Prot, Gold Bull. **41**, 105 (2008).

[53] M. Rashidi-Huyeh, S. Volz, and B. Palpant, Phys. Rev. B **78**, 125408 (2008).

[54] M. Rashidi-Huyeh and B. Palpant, Phys. Rev. B **74**, 075405 (2006).

[55] Y. Guillet, M. Rashidi-Huyeh, D. Prot, and B. Palpant, Gold Bull. **41**, 341 (2008).